Analysis and Efficient Design of Sub-THz Transmitarrays with Three Anisotropic Layers

Orestis Koutsos[1,2], Francesco Foglia Manzillo[1], Antonio Clemente[1], Ronan Sauleau[2]
[1] Univ. Grenoble Alpes, CEA, Leti, 38000 Grenoble, France
{orestis.koutsos, francesco.fogliamanzillo, antonio.clemente}@cea.fr
[2] Univ Rennes, CNRS, IETR (Institut d'Électronique et des Technologies du numéRique) - UMR CNRS 6164, F-35000 Rennes, France, ronan.sauleau,@univ-rennes1.fr, orestis.koutsos@etudiant.univ-rennes1.fr

***Abstract*—In this paper, we study the transmission behavior of a three-layer architecture comprising anisotropic FSS layers with applications to the optimal design of transmitarray (TA) antennas. We employ a theoretical analysis considering the depolarizing properties of the middle layer. We derive a condition showing that we can cover the full phase of transmission achieving at the same time zero insertion loss (IL). Lastly, a 3-bit 40×40 TA is realized at 300 GHz, based on the previous analysis. The antenna is able to attain a maximum gain of 35.1 dBi with an aperture efficiency of 64.8%, which is only 0.5 dB less than the ideal case of a TA with full transmission and perfect phase compensation.**

***Index Terms*—transmitarray, unit-cell, anisotropic FSS, rotator.**

I. Introduction

In the frame of beyond 5G communications, the use of high gain antenna systems has become a necessity. Phase-shifting surfaces (PSS) such as reflectarrays (RA) and transmitarrays (TA) have been of great interest, as they combine the concepts of aperture antennas and phased arrays keeping the favorable features of both.

TA antennas have already proven to be suitable at frequencies below 100 GHz [1] and can be designed to achieve a relatively low profile [2]. At very high frequencies, the fabrication process of the phase-shifting elements, called unit-cells, might become prohibitive, especially when a fine phase resolution is targeted considering a low-cost technology. Different solutions have been suggested, including the combination of different unit-cell architectures [3] or the use of stacked frequency-selective-surfaces (FSSs) [4].

The main objective for the TA is to cover the full circle of transmission phase (360°) and exhibit near-zero IL. A theoretical approach relating the impedance sheets of multilayer FSSs to the phase coverage was presented in [5]. The authors proved that for any symmetrical FSS comprising identical equally-spaced impedance sheets, at least three layers are necessary to cover the full phase range achieving an insertion loss lower than 3 dB. A slight improvement in terms of maximum insertion loss is possible if we consider three non-identical layers [6].

Even though the property of symmetry is generally a positive feature, it represents a constraint on the maximum capabilities of a single FSS for the transmission phase coverage. In this contribution, we consider a unit-cell that comprises three anisotropic FSS layers. The outer layers are orthogonal polarization grids, while the middle layer is a polarization rotator. This configuration has already been employed for TA applications [7] at high frequencies, showing promising results in terms of phase coverage and broadband frequency behavior. In section II we focus primarily on the middle impedance sheet in order to make clear the operation of the unit-cell and to optimize the phase coverage and insertion loss. Based on the concept of transformation electromagnetics (TrEM) [8] the properties of the rotator are expressed as a pair of decoupled admittance values. Then, using a cascaded sheets method [9] we present the transmission behavior of the unit-cell as a function of the two admittance values of the rotator, proving that the unit-cell can achieve any transmission phase and zero IL. Lastly, in section III we realize a TA antenna operating at 300 GHz, showing that it can be possible to design a near-perfect discrete lens with very high aperture efficiency, even using low-cost fabrication technologies. We also relate the TA phase distribution to a pair of admittance maps that describe the rotator. The proposed unit-cell and design procedure are very attractive as they allow one to control the transmission properties by optimizing a single impedance layer (the rotator).

II. Study of the unit-cell

A. Theoretical analysis

The architecture under analysis is shown in Fig. 1. It comprises three non centro-symmetric FSS layers, spaced by dielectric slabs of permittivity ε_r. The outer layers are orthogonal grid polarizers and the middle layer is a polarizing rotator, usually a skewed dipole type, like in our example ($Iota$ shape dipole). For simplicity, the two polarizers have the same features and only differ for their orientation of their strips.

Considering a linearly polarized wave, we can define two principle states, namely TE and TM along the x and y axis, respectively, based on the electric field. We assume that the wave propagates along the z-axis and it is normally incident to the structure. Furthermore, we consider for simplicity that all materials of the unit-cell are lossless and each FSS is reciprocal.

Now, let's assume that an x-polarized wave is incident from the left side of the unit-cell. The rotator will depolarize the incident wave, resulting into four emergent waves inside the structure, x- or y-polarized, propagating along $\pm\hat{z}$. The two

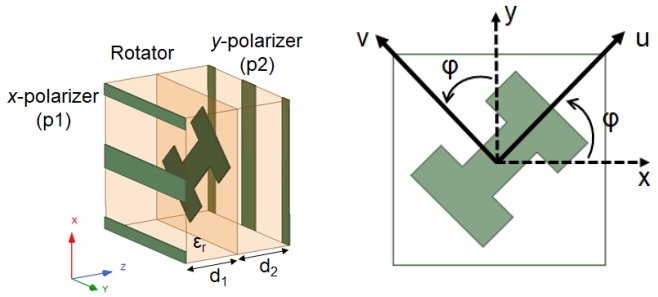

(a) (b)

Fig. 1: (a) Proposed unit-cell with 3 metallic layers, M1, M2 and M3. (b) Rotator configuration, used as a reference. The (x,y) is the unit-cell global system and the (u,v) is the crystal system related to the middle layer.

polarizers create a cavity effect, trapping the waves between them, leading to multiple internal reflections. Eventually, if the unit-cell thickness and the rotator's properties are chosen correctly, we will get a y-polarized wave, transmitted to the other side of the unit-cell, ideally exhibiting zero IL. Due to the asymmetry of polarization to the two sides of propagation, this structure can be referred to as asymmetric linear polarizer (ALP). Each sheet of the ALP exhibits a different response for each state of polarization. Consequently, we must utilize both states in order to describe the full problem and discuss the effect of anisotropy on the transmission behavior.

Each FSS, due to its sub-wavelength thickness, can be treated as an artificial boundary expressed by certain effective surface parameters [10]. Therefore, it is approached as an electric sheet with a constant value of admittance. In general, the admittance is a 2×2 matrix, considering two states of polarization:

$$\overline{\overline{Y}}^{XY}_{FSS} = \begin{bmatrix} Y^{xx} & Y^{xy} \\ Y^{yx} & Y^{yy} \end{bmatrix} \tag{1}$$

where $Y^{xy} = Y^{yx}$ for the reciprocal FSS. If we know the admittance properties of each FSS, we can calculate the S parameters of the entire unit-cell by considering a method of cascaded sheets, as explained in [9]. Specifically, we calculate the 4×4 equivalent transfer matrix using the expression:

$$\begin{bmatrix} \mathbf{A} & \mathbf{B} \\ \mathbf{C} & \mathbf{D} \end{bmatrix}_{FSS} = \begin{bmatrix} \mathbf{I} & \mathbf{0} \\ \mathbf{nY}_{FSS} & \mathbf{I} \end{bmatrix} \tag{2}$$

where $\mathbf{I}$ is the unitary matrix and $\mathbf{n}$ is the 90° rotation matrix. The dielectric is expressed as a transmission line with specific length and characteristic impedance. By cascading all the transfer matrices, we can calculate the global transfer matrix of the unit-cell and establish a relationship between the $ABCD$ elements and the S parameters. The transmission coefficient will be a function of all the admittances of each FSS.

In the case of polarizers, if they are aligned with the x and y axes, the matrix will be diagonal ($Y^{xy} = Y^{yx} = 0$). However, the rotator requires three variables to describe entirely the anisotropic behavior. If we try optimizing three parameters of the same layer to achieve multiple phase-shifting unit-cells, the analysis can become complicated. Essentially, we will have to rely on full-wave parametric simulations to mitigate the issue. Instead of that, we propose here a straightforward procedure for a fast and optimal design of the necessary rotators to simplify the problem and meet the TA criteria. The proposed approach is based on the concept of transformation electromagnetics (TrEM), a mathematical approach that translates the material parameters of a structure from one coordinate system to a new one.

Based on the latter, we consider a two-dimensional transformation of the FSS from an (x,y) to a (u,v) system, as shown in Fig. 1b. Additionally, we define a coordinate system, also called Crystal system, in which the admittance matrix of the layer can be diagonal. In our example, we assume that the Crystal system is the (u,v). Therefore, the equivalent admittance matrix can be expressed as:

$$\overline{\overline{Y}}^{UV}_{FSS} = \begin{bmatrix} Y^u & 0 \\ 0 & Y^v \end{bmatrix} \tag{3}$$

Initially, we assume that the crystal axes overlap the (x,y) system and the dipole element is aligned with the x axis. Afterwards, we rotate the entire FSS by some angle ϕ in order to get the configuration of Fig. 1b. It can be proved [8] that the value of the FSS admittance in the (x,y) is related to the admittance value of the crystal system as:

$$\overline{\overline{Y}}^{XY}_{FSS} = \frac{\overline{\overline{J}}\,\overline{\overline{Y}}^{UV}_{FSS}\,\overline{\overline{J}}^{T}}{|\overline{\overline{J}}|} \tag{4}$$

where $\overline{\overline{J}}$ is the Jacobian of the transformation. For our case, the Jacobian is the rotation matrix R and the expression of the anisotropic admittance of eq. (1) will be:

$$\overline{\overline{Y}}^{XY}_{FSS} = R(\phi)\overline{\overline{Y}}^{UV}_{FSS}R^T(\phi) \tag{5}$$

The rotator properties are now related to a pair of admittance values and one angle of rotation. We can calculate the values of the Crystal system using the following expression [9]:

$$\overline{\overline{Y}}^{UV}_{FSS} = -\frac{2}{\eta}\mathbf{S}_{11}(\mathbf{I}+\mathbf{S}_{11})^{-1} \tag{6}$$

where $\mathbf{S}_{11}$ is the 2×2 reflection coefficient matrix calculated at the crystal axes and the layer is embedded between the same material ($\eta = \eta_0/\sqrt{\varepsilon_r}$).

We can further study the angle of rotation by focusing on the depolarization factor. This coefficient is zero when considering the Crystal system, but it exhibits a certain value if we rotate the FSS. We can use eq. (5) and eq. (6) to calculate the transmission coefficient of an arbitrary anisotropic FSS as a function of Y^u,Y^v and ϕ. Focusing on the depolarization factor, we get eventually the following expression:

$$S^{yx}_{21} = sin(2\phi)\frac{Y^u - Y^v}{(Y^u + 2/\eta)(Y^v + 2/\eta)} \tag{7}$$

It is clear that for any pair of Y^u,Y^v the maximum magnitude of this coefficient is found when $\phi = \pm 45°$, which is in agreement with the existing designs. For the rest of the study,

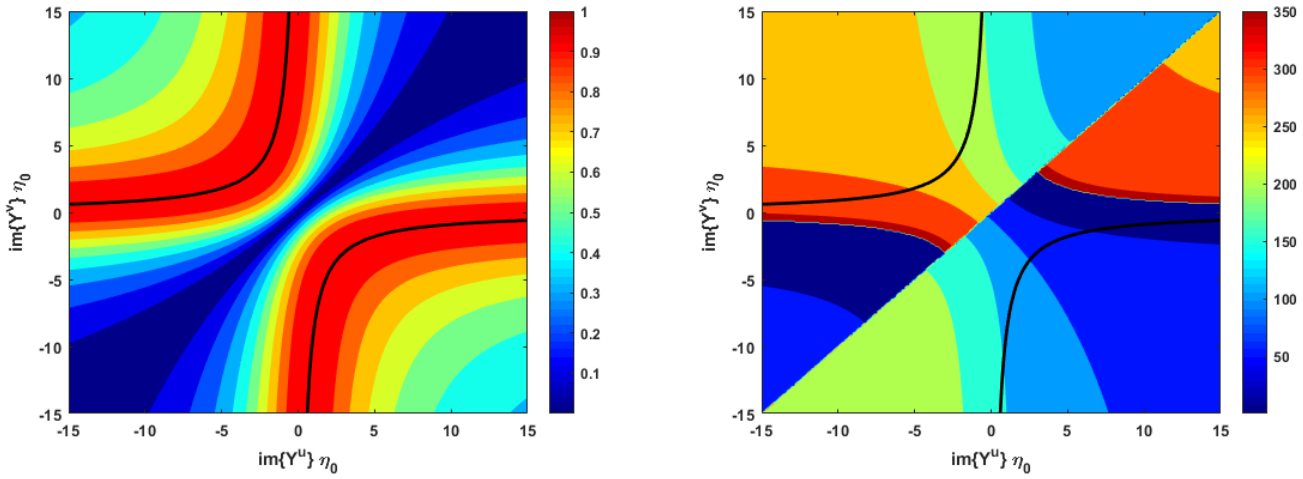

(a) (b)

Fig. 2: Magnitude (a) and phase (b) of transmission coefficient T_{yx} of the studied unit-cell as a function of the rotator's properties, considering ideal polarizers and dielectric thickness $\lambda_{\varepsilon_r}/4$ between the layers. The selected permittivity is $\varepsilon_r = 3$. The dark solid line represents the values for perfect matching (zero insertion loss) from eq. (10).

we will consider that the angle of rotation is set for the maximum depolarization. We must emphasize that the wave is normally incident to the unit-cell and the transformation of the middle layer does not affect the surrounding material.

B. Design procedure

Before we focus on the rotator properties, we study first the rest of the structure, i.e. the polarizers and the dielectric properties. These elements are responsible for the cavity effect which is crucial to the unit-cell behavior. It can be found [7] that the optimal distance between the rotator and each polarizer should be close to $\lambda_{\varepsilon_r}/4$, where λ_{ε_r} is the wavelength inside the dielectric.

We can facilitate the study if we assume that each polarizer is ideal. This simply means that they are either fully transparent or fully reflective, depending on the polarization. In terms of admittance, based on Fig. 1, the respective values are:

$$Y_{p1}^{x} = 0 \quad , \; Y_{p1}^{y} \to \infty \tag{8}$$

$$Y_{p2}^{x} \to \infty \quad , \; Y_{p2}^{y} = 0 \tag{9}$$

In reality, we will need to consider a relatively small capacitive and a finite inductive effect for each case. For configurations such as the illustrated grids, the reflective case is almost ideal. We can compensate with the small capacitance by slightly reducing the thickness. The scattering behavior of the grids has been thoroughly studied [11] and there is plenty of work to rely on their design and optimization as polarizing structures.

Using the analysis method discussed in II-A, we can calculate the expression of the unit-cell transmission coefficient T^{yx} as a function of the two unknown variables, Y^u and Y^v. The results calculated for a center frequency f_0, having ideal polarizers and the middle layer rotated by $45°$, are shown in Fig. 2. Considering the first graph, it is clear that under a certain condition between the two admittance values, we can get a perfect transmission without any IL. Focusing only on this pair of values, we eventually find that the relationship, depicted with a dark solid line, is:

$$Y^u Y^v = (\varepsilon_r/\eta_0)^2 \tag{10}$$

where η_0 is the characteristic wave impedance of vacuum, surrounding the unit-cell. Additionally, based on the second graph, we can see that if we move along the curve of eq. (10), the phase of transmission will range from 0° to 360°. In other words, we will cover the full phase of transmission (360°) exhibiting zero IL. This is the best case scenario that one can think of in the context of TA applications. If, for instance, we consider a TA with 3-bit phase resolution, we can simply move along the curve and pick 8 pairs with $45°$ relative phase difference. The result of this will be an array of perfect wavefront control at the frequency of interest.

An interesting observation is that, in order to satisfy the matching condition of eq. (10), the rotator must exhibit purely capacitive and purely inductive properties for each polarization, respectively, considering the crystal axes. In practice, we can only obtain finite values of admittances. Based on the second graph of Fig. 2, in order to retrieve a transmission with $0°$ or $180°$ of phase, we need to find a rotator exhibiting an infinite value of admittance for one state of polarization. Of course, for a realistic scenario this is not possible. Instead, we will need to introduce a small phase error for the $0°$ and $180°$ phase-states of unit-cells, if we consider a TA with high phase resolution. Nevertheless, this might not affect the design, as the unit-cell would still exhibit 0 IL and the phase error could be relatively small, depending on the maximum value that we are able to obtain from the FSS.

Lastly, considering the design approach, we can emphasize two points. First of all, we need to modify only the middle layer in order to realize multiple phase-states, which makes

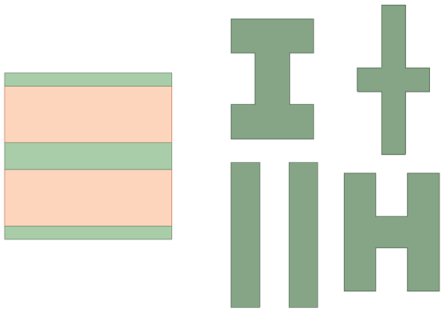

Fig. 3: Realized scenario of ALP unit-cells considering one type of polarizer and four rotators for a 3-bit phase quantization, including the mirrored cases (90° rotation).

this concept appealing to any fabrication process. Secondly, if we focus on N configurations of rotators, we can obtain $2N$ phase states, because by mirroring the middle layer (rotation by $-45°$) we get a difference of $180°$ in the phase of transmission with respect to the initial case.

III. Application to Transmitarray Design

In order to highlight the positive features of the study presented in section II, we synthesize a TA antenna that operates at 300 GHz. As an example, we consider a 40×40 elements array, with unit-cell size of $\lambda/2$ (0.5 mm at 300 GHz). The array is illuminated by a cosine type focal source of 10 dBi gain and $65.6°$ of half-power beamwidth (HPBW). An ad-hoc numerical tool is used [1], in order to calculate the optimal focal distance and phase distribution in terms of maximum gain and aperture efficiency. For the ideal scenario (perfect phase compensation and 0 IL), we get F = 10 mm (F/D = 0.5), with 35.6 dBi maximum gain and 72% aperture efficiency.

In order to consider a realistic approach, we use real polarizers, as shown in Fig. 3. The width of each strip is $W = 80\ \mu m$ and the gap is $G = 170\ \mu m$, leading to a filling factor of $F = W/(W+G) = 0.32$. The two polarizers, when placed between vacuum and a dielectric of permittivity $\varepsilon_r = 3$, they exhibit admittance values equal to $Y^x_{p1} = Y^y_{p2} = j0.3/\eta_0$ and $Y^y_{p1} = Y^x_{p2} = -j5.4/\eta_0$ at 300 GHz. To compensate with those values, we reduce the thickness of the dielectric to $0.22\lambda_{\varepsilon_r}$. This leads to a slight IL of 0.25 dB in the matching case.

Due to the mirroring effect, we can limit the window of observation to the fourth quarter of the graph. Considering a 3-bit scenario, we need 4 pairs of admittances and $45°$ of relative phase difference between the unit-cells. The other four pairs are calculated as $Y^u = Y^v$ and $Y^v = Y^u$, imposing a rotation of $\phi = -45°$ on the rotator and looking at the second quarter of the graph. Furthermore, we design 4 types of rotators, as shown in Fig. 3. Their dimensions were set to meet the criteria of the PCB technology. The admittance values of the 3-bit scenario for both cases, theoretical analysis and realized rotators, are shown in Fig. 4, along with the curves that describe the minimum IL condition, one with ideal

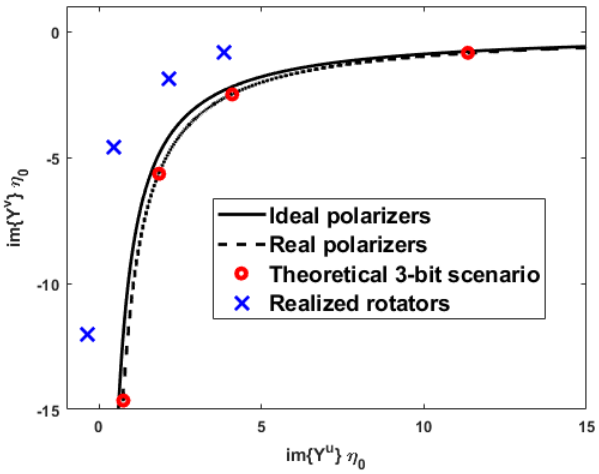

Fig. 4: Results of the admittance values of the rotator, imposing a condition of minimum IL. In the dark solid line the IL is 0 dB, while in the dashed one it is 0.25 dB, considering real polarizers. The four red dots are calculated based on the theoretical analysis and they are placed upon the dashed line. The blue crosses are the equivalent values of the realized rotators of Fig. 3.

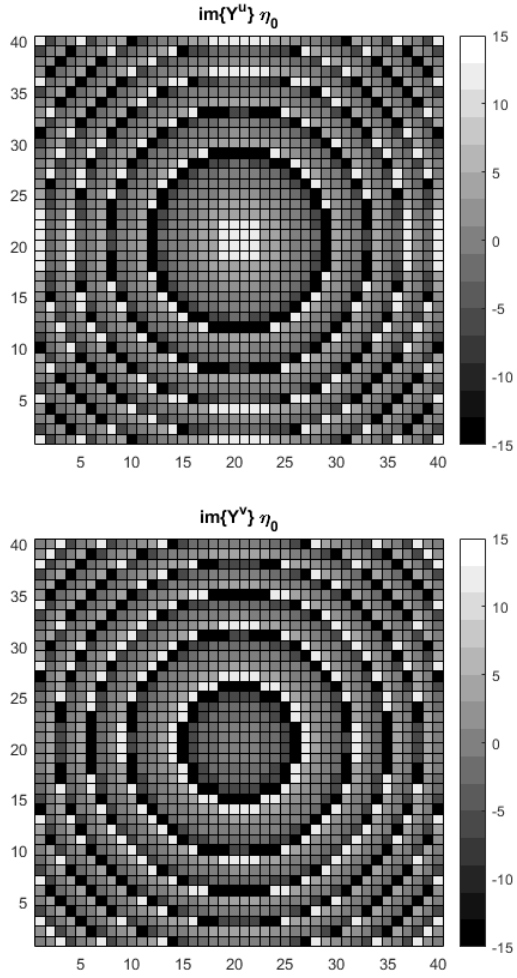

Fig. 5: Admittance map of the rotator calculated from the study of section II. The rotator is placed at $45°$ or $-45°$ at each unit-cell.

TABLE I: Comparison table between the study of section II and a realized scenario.

Unit-cell S-parameters	**Theoretical study II**				**Realized scenario (Fig. 3)**			
Targeted phase (°)	**Phase (°)**	**IL (dB)**	**Im$\{\mathbf{Y}^{u,v}\}\eta_0$**		**Phase (°)**	**IL (dB)**	**Im$\{\mathbf{Y}^{u,v}\}\eta_0$**	
35	35	0.25	11.35	-0.85	58	0.89	3.854	-0.83
80	80	0.25	4.1	-2.5	90	1.16	2.17	-1.86
125	125	0.25	1.85	-5.65	140	1.4	0.44	-4.58
170	159	0.25	0.75	-14.65	174	1	-0.36	-12

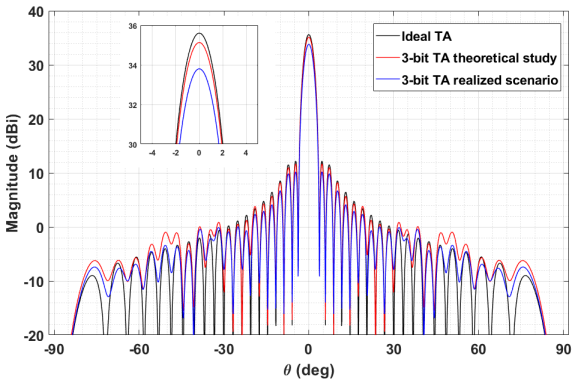

Fig. 6: Radiation pattern of the $\phi = 0°$ plane at 300 GHz for three scenarios.

and one with real polarizers. We can further see that the compensation of the width has been successful with respect to the ideal case. Table I shows also a comparison of the main parameters. Considering the realized rotators, if we compare the IL graph of Fig. 2a to the admittance data of Fig. 4, we can see that they move along the curve of 1 dB IL.

We can synthesize a real TA by considering two maps of admittance that describe the middle layer at the crystal axes, as shown in Fig. 5. For each calculated point, the rotator is placed at $45°$ or $-45°$ with respect to the center of each respective unit-cell. The equivalent admittance maps of the two polarizers are constant along the entire surface and thus they are omitted. This is a useful and simple method to design a real array that comprises only 3 metal layers in which we need to modify only one of them and minimize the backscattering effect.

Lastly, the radiation pattern at 300 GHz for the three cases (ideal TA, theoretical design, realized rotators) is plotted in Fig. 6. For the theoretical, 3-bit case scenario, we get a maximum gain of 35.1 dBi and 64.8% aperture efficiency, taking into account 0.25 dB IL and a slight phase error of $11°$ at one phase-state. The gain loss of the theoretical antenna is only 0.5 dB with respect to the ideal case. Finally, the array comprising realized rotators exhibits 33.7 dBi and 46.5%, respectively, which is due to the average 1 dB IL and the existence of some relative phase error between the phase states.

IV. Conclusion

In this study, we examined the case of a 3-FSS unit-cell, called ALP, comprising anisotropic elements for TA applications. The theoretical analysis showed that the configuration can cover all the phase range of transmission with zero or negligible IL, considering ideal or real polarization grids, respectively. We demonstrated the effectiveness of the proposed procedure by designing a 300 GHz TA antenna with four types of rotators. Even using a simple PCB technology with a minimum resolution of 80 μm, the rotator admittances approach the optimal values, determined by means of the proposed design procedure. The gain of the designed antenna is 1.4 dB less than the maximum achievable value.

Acknowledgment

This work was partly supported by the National Research Agency (ANR) through the project "Next5G" under Grant ANR 18-CEA25-0009-01.

References

[1] H. Kaouach, L. Dussopt, J. Lanteri, T. Koleck, and R. Sauleau, "Wideband low-loss linear and circular polarization transmit-arrays in V-band," *IEEE Trans. Antennas Propag.*, vol. 59, no. 7, pp. 2513–2523, Jul 2011.

[2] M. Smierzchalski, A. Clemente, M. Huchard, and C. Barbier, "Wideband low-profile transmitarray antenna for backhauling at 60 GHz," in *12th Eur. Conf. Antennas Propag. (EuCAP 2018)*, 2018, pp. 1–5.

[3] F. Foglia Manzillo, A. Clemente, and J. L. González-Jiménez, "High-gain D-band transmitarrays in standard PCB technology for beyond-5G communications," *IEEE Trans. Antennas Propag.*, vol. 68, no. 1, pp. 587–592, 2020.

[4] S. Qu and H. Yi, "Low-cost two-layer terahertz transmitarray," in *2017 International Applied Computational Electromagnetics Society Symposium (ACES)*, 2017, pp. 1–2.

[5] A. H. Abdelrahman, A. Z. Elsherbeni, and F. Yang, "Transmission phase limit of multilayer frequency-selective surfaces for transmitarray designs," *IEEE Trans. Antennas Propag.*, vol. 62, no. 2, pp. 690–697, Feb 2014.

[6] J. Luo, F. Yang, S. V. Hum, S. Xu, and M. Li, "Study of a low-profile transmitarray element using 3 non-identical layers," in *2018 IEEE MTT-S International Wireless Symposium (IWS)*, Chengdu, 2018, pp. 1–3.

[7] L. Marnat, K. Medrar, and L. Dussopt, "Highly integrable high gain substrate-integrated planar lens for wide D-band applications," in *2020 14th Eur. Conf. Antennas Propag. (EuCAP)*, 2020, pp. 1–4.

[8] A. M. Patel and A. Grbic, "Transformation electromagnetics devices based on printed-circuit tensor impedance surfaces," *IEEE Trans. Microw. Theory Tech.*, vol. 62, no. 5, pp. 1102–1111, 2014.

[9] C. Pfeiffer and A. Grbic, "Bianisotropic metasurfaces for optimal polarization control: Analysis and synthesis," *Phys. Rev. Applied*, vol. 2, p. 044011, Oct 2014.

[10] Y. Vahabzadeh, N. Chamanara, and C. Caloz, "Generalized sheet transition condition FDTD simulation of metasurface," *IEEE Trans. Antennas Propag.*, vol. 66, no. 1, pp. 271–280, 2018.

[11] M. Ando and Ken Takei, "Reflection and transmission coefficients of a thin strip grating for antenna application," *IEEE Trans. Antennas Propag.*, vol. 35, no. 4, pp. 367–371, 1987.